

Appearance of Midair plasma extenuation of Shock Wave

G.Harikrishnan, Seethalakshmi.S

Department of Physics, Kalasalingam University, Krishnankoil

Abstract

Shock wave is a detriment in the growth of supersonic aircrafts; it rises flow drag as well as external heating from extra friction; it similarly initiates sonic boom on the ground which prevents supersonic jetliner to fly overland. A shock wave extenuation method is established by experiments directed in a Mach 2.5 wind tunnel. Non-thermal air plasma produced symmetrically in obverse of a wind tunnel perfect and upstream of the shock, by on-board 60 Hz episodic electric discharge, works as a plasma deflector, it bounces received flow to alter the shock from a well-defined involved shock into a extremely curved shock structure. In a sequence with growing discharge intensity, the altered curve shock growths shock angle and changes upstream to become separate with growing standoff distance from the model. It develops diffusive and evaporates near the top of the discharge. The flow deflection growths the equivalent cone angle of the model, which in essence, decreases the corresponding Mach number of the received flow, establishing the discount of the shock wave drag on the cone. When this corresponding cone angle exceeds a dangerous angle, the shock develops detached and fades away. This shock wave mitigation method helps drag discount as well as removes sonic boom.

Keywords - Shock Wave Mitigation, Electric Discharge, Air Plasma Deflector, Shadowgraph, Drag Reduction, Wind Tunnel, Charge Transfer.

I. INTRODUCTION

Shock wave seems in the procedure of a steep pressure gradient. Once a supersonic flow is glanced by an object, e.g., a spacecraft, the airflow disturbances cannot catch up after the object. These disturbances coalesce into a shock wave to introduce a discontinuity in the flow properties at the shock obverse location, where is the accessible edge of deflected flow turbulences from the object. Shock wave growths the pressure in front of the thing, producing important improvement of the movement drag and resistance on the object. Furthermore, unsteady shock wave in supersonic flight goods notorious sonic prosperous on the ground. A physical spike is presently used in a supersonic spacecraft to move unique bow shock upstream from the blunt-body nose site to its tip site in the novel procedure of a conical oblique shock to alleviate shock things on the flight. Thermal energy statement in front of a flying body to trouble the incoming flow and shock wave formation has been studied. The heating of the

supersonic received flow results in a local discount of the Mach number, which weakens shock wave and growths the shock angle. It is an real approach to decrease the wave drag and shock noise in supersonic and hypersonic flows, though, the energy gain from drag discount is much less than the injected heating energy. Nevertheless, this is a possible method for sonic boom attenuation.

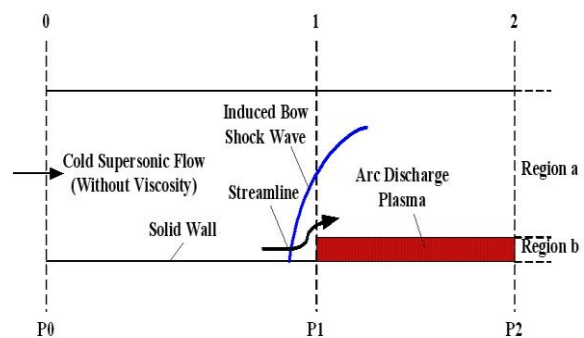


FIG 1 Investigation shock wave

Plasmas alteration of the shock structure has been evidenced in a number of shock-tube experiments. Plasma can efficiently change electric energy to thermal energy for air heating. Furthermore, it has the potential to possibly propose a non-thermal alteration result on the structure of shock waves. The results showed an increased velocity and dispersion on shock waves spreading in the glow release region. Though, the main inspiration for the study of plasma effects on shock waves is attributed to the observation of a wind tunnel research accompanied by Gordeev et al. High-pressure metal vapor plasma, produced inside the chamber of a cone-cylinder perfect by exploding wire off electrical short circuit, was inserted into the supersonic flow done a nozzle. An important drag decrease was measured, which was too big to be accounted for by the thermal effect alone. In a following wind tunnel experiment, the shock front improved dispersion in its structure in a moldering electric discharge plasma was identified. Implement a plasma torch component in a cone-shape wind tunnel model for on-board periodic electric discharges, the result of a series of wind channel experiments presented that the shock front increased dispersion in its structure and/or standoff detachment from the model when plasma was generated ahead of a model. The separate curve shock increased shock angle and faded gone as the discharge was deepened. This cone model was

truncated to represent a blunt body. The experiment presented that on-board pulsed electric releases transformed the baseline bow shock to an involved oblique shock. Computational and experimental studies designate that an added magnetic field can toughen the arc plasma to additionally weaken the shock wave. On the other hand, microwave plasma projected on-board was exposed still too weak to introduce any noticeable result on the shock wave in a hypersonic flow.

II. EXPERIMENTAL SETUP

Experiments were accompanied in the test section, with a $0.38 \text{ m} \times 0.38 \text{ m}$ cross section, of a supersonic blow-down wind tunnel, shown in Figure 2. The upstream airflow had a flow speed $v = 570 \text{ m/s}$, temperature $T_1 = 135 \text{ K}$, and a pressure $P_1 = 0.175 \text{ atm}$.

A. Wind Tunnel Model

The wind tunnel typically has a truncated-cone body linked to a cylindrical body devoted to a container. It also contains an improved solid tungsten rod of a diameter $d = 2.4 \text{ mm}$, detained by a ceramic insulator, in residence concentrically with the truncated-cone body to form the electrodes for the discharge. The cone-shaped earthenware insulator composed with the tungsten rod set as a small protruding spike substitutes the shortened part of the cone. The schematic of the model is obtainable in Figure 3. The shortened 60° cone has a frontal diameter $D = 11.1 \text{ mm}$ and a height $L = 12.7 \text{ mm}$. The cylindrical base of the cone has a diameter $D_b = 25.4 \text{ mm}$. The distance from the tip to the edge of the truncated-cone surface is about 5 mm .

B. Periodic Discharge

A half-wave corrected 60 Hz power supply was used for interrupted discharge. The wind tunnel model is grounded and the spike is linked to the negative output voltage of the power supply. The discharge recruits in the region near the tip of the spike, where focused electric field pushes produced electrons to the upstream region. The produced spray-like plasma shown in Figure 4 acted as a spatially distributed deflector, which deflected the received flow.



FIG 2 Mach 2.5 wind tunnel for performing the experiment

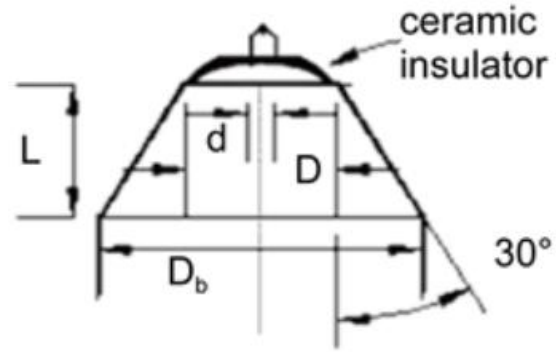


FIG 3 schematic of the wind tunnel model implemented with electric discharge electrodes for plasma generation



FIG 4 Photo of the arc discharge in a supersonic flow.

C. Optical Diagnostics

Shadowgraph technique was used to optically identify the flow field around the spike and nose of the cone. A black and white (BW) charge coupled device (CCD) camera, with a frame rate of 30 frames per second and exposure time of $1/60 \text{ s}$ (which is slightly less than four times of each discharge period), was used to record straight the shadowgraph images of the flow dynamics. A video (color CCD) camera as the compatible one to the BW CCD camera was cast off to record the spatial delivery and progressive development of the plasma glow with the similar frame rate and experience time. The video graph recorded in each frame is an integrated result over the exposure time, and thus the progressive variation of the shock wave assembly and plasma glow through a single discharge period cannot be recorded directly. Continuous video graph of the flow can still reveal significant information regarding the dynamic performance of the flow field when two consecutive frames can be extracted since the discharge does not have a constant period. Furthermore, the results extracted from videotapes recording the shadowgraph images of the flow and plume images of plasma can deliver the association among the plasma delivery and the alteration of the shock structure. It assists to deduce necessary plasma conditions to

attain important plasma consequence on the shock wave.

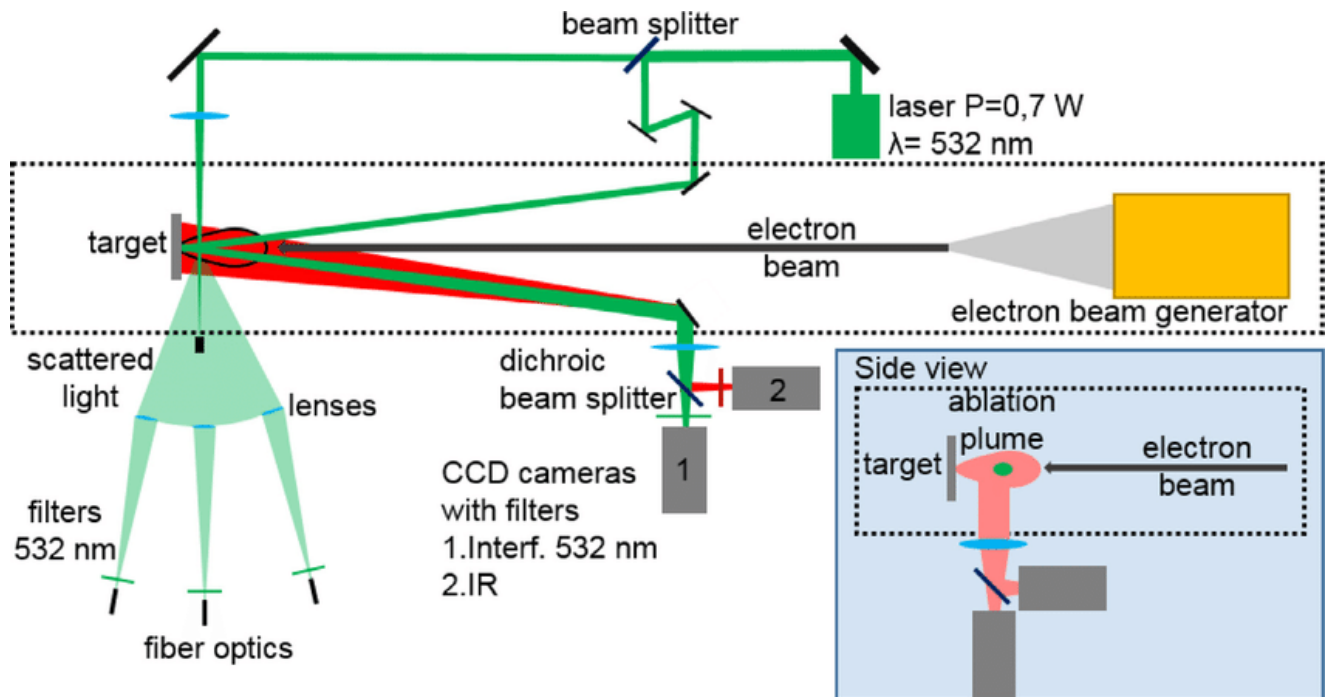


FIG 5 Schematic of optical diagnostics

1. The Shadow Imaging System

A schematic of the optical arrangement for immediate Shadow and Plasma Glow/Afterglow video imaging is shown in Figure 6. Anglowing lamp with beam-forming optics and filters was used for the current described clarifications. A parabolic mirror, of diameter 0.3 m and central length of 3.7 m , collimated the divergent beam from the (point) light source before it approved finished the wind tunnel test section windows. On the other side of the wind tunnel, an image creating optics, containing of a lens and a

B&W high determination CCD camera, was used to find the Shadow images. The Shadow images were predictable straight on the CCD area, escaping the use of projection screens, and recorded at a rate of 30 frames/sec with an exposure time of $1/60\text{ sec}$. The image exaggeration could be adapted in the range $0.1 - 0.5\text{ mm/pixel}$ by camera positioning along the optical axis. Neutral density filters were used to cut down light concentration coming from the flow itself, prompted by the discharge.

2. The Plasma Glow/Afterglow Imaging System

For plasma imagining, we used a color CCD camera located on whichever side of the wind tunnel, at a minor angle with admiration to the optical axis of the scheme. This videocamera recorded at a rate of 30 frames/sec with selectable exposure time from $1/60$ to $1/4000\text{ sec}$. A neutral density filter was practical to the CCD camera for

reducing the airglow concentration of the release entering the camera. The synchronization among Shadow and plasma glow recorded images was understood by post-processing of the conforming images (based on the release glow that has temporal determination of less than 100 msec). Following of video frames presented that the frame synchronization error between cameras during one-run duration ($100 - 300\text{ surrounds}$) was less than half frame that was less than $1/60\text{ sec}$.

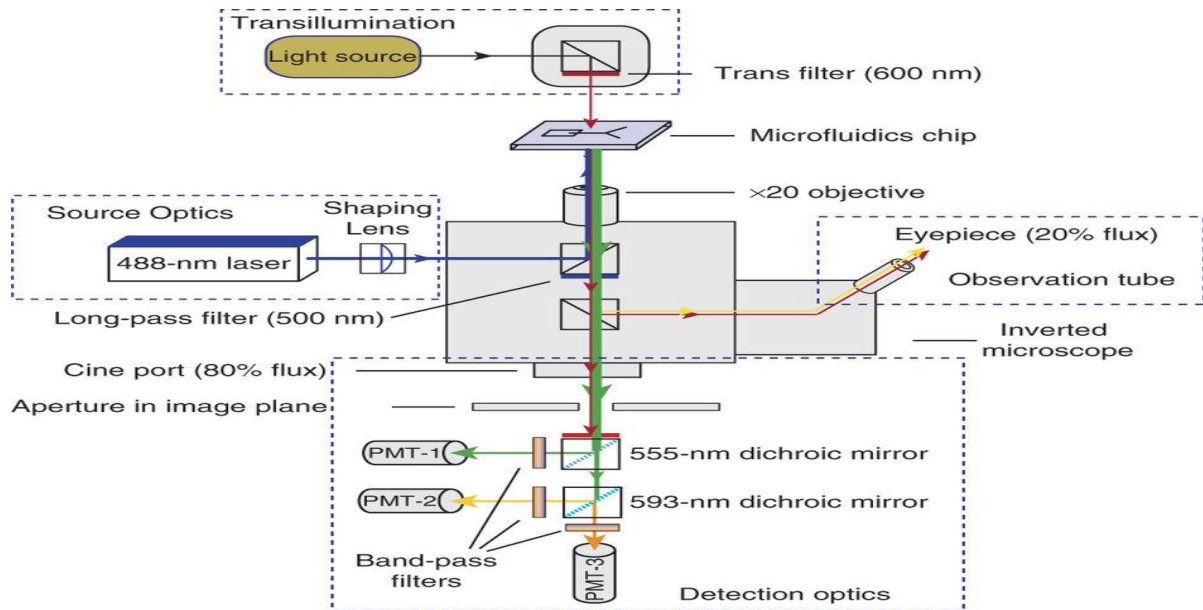


FIG 6 schematic of an optical setup

IV. EXPERIMENTAL RESULTS

The modification consequence depended on the density and volume of the plasma deflector produced through each release, which is in small pulse. This time variable deflector caused the shock structure and its obverse location to vary in time. Though the temporal difference of the shock wave structure through a single discharge period could not be recorded straight, the wanted information concerning the fleeting performance of the movement field was exposed in both pair of successive frames removed from the nonstop shadow graph of the flow. This is established in Figure 7, which includes a sequence of four pairs of shadowgraphs presentation the recapping response of the shock wave to the plasma deflector. In this and other shadowgraphs and plasma plume images presented later, the flow is from left to right. In Figure 7, the shadowgraphs in the left panel show a steady state baseline shock produced in front of the wind tunnel model. The plasma effect on the baseline shock is then shown by the shadowgraphs in the right panel, in which both one is a following video frame to the one on the left. Because of the difference of the initial time of each discharge, the dissimilar alterations of the shock structure shown in the right panel shadowgraphs obvious the dependence of the shock wave mitigation on the intensity of the plasma deflector. As seen, the baseline shock is divided into two, with a new one moved upstream; the original baseline shock becomes exact weak and the new one is a curved one with superior shock angle. As the curved shock front moves upstream, it develops diffusive with cumulative shock angle. It is finally removed

and the unique baseline shock spreads out becoming expansion waves.

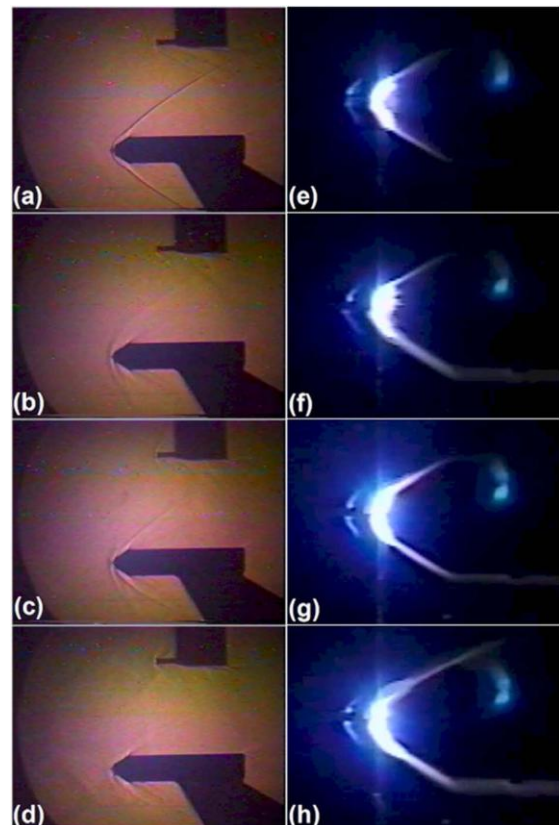


FIG 7 An assembled time sequence of four shadowgraphs (a)-(d) to represent the flow response to the plasma deflector (e)-(h) during one discharge period in the middle of a wind tunnel run at Mach 2.5.

V. CONCLUSIONS

The wave drag of the shock on the cone depends on the strength of the shock, which in turn depends on the Mach numeral of the movement. It is originate that the effective Mach number $M1(\xi)$ of the deflected flow in the tip area of the wind tunnel typical is lesser than $M10 = 2.5$. A reduction in the real Mach number of the entering flow in the tip area confirms that this air plasma deflector can indeed decrease the wave drag of the shock on the cone. Furthermore, the altered shock structure changes upstream gone from the cone; it also outcomes to the discount of the wave drag on the cone. The new results conclude that it is practicable to apply a non-thermal air plasma deflector for the attenuation or ideal removal of shock wave expansion around a supersonic vehicle. The expected results of condensed fuel consumption and having slighter propulsion system necessities, for the similar cruise speed, will main to the understandable commercial increases that contain larger payloads at smaller take-off gross weights and broadband shock noise suppression through supersonic flight.

REFERENCE

- [1] Chang, P.K. (1970) Separation of Flow. Pergamon, Oxford.
- [2] Riggins, D., Nelson, H.F. and Johnson, E. (1999) Blunt-Body Wave Drag Reduction Using Focused Energy Deposition. AIAA Journal , 37, 460-464.
- [3] Schülein, E. and Zheltovodov, A. (2011) Effects of Steady Flow Heating by Arc Discharge Upstream of Non-Slender Bodies. Shock Waves , 21, 383-396. <http://dx.doi.org/10.1007/s00193-011-0307-1>
- [4] Markhotok, A. (2015) A Mechanism of Wave Drag Reduction in the Thermal Energy Deposition Experiments. Physics of Plasmas , 22, 063512. <http://dx.doi.org/10.1063/1.4922434>
- [5] Gordeev, V.P., Krasilnikov, A.V., Lagutin, V.I. and Otmennikov, V.N. (1996) Plasma Technology for Reduction of Flying Vehicle Drag. Fluid Dynamics , 31, 313-317. <http://dx.doi.org/10.1007/BF02029693>
- [6] Baryshnikov, A.S., Basargin, I.V., Dubinina, E.V. and Fedotov, D.A. (1997) Rearrangement of the Shock Wave Structure in a Decaying Discharge Plasma. Technical Physics Letters , 23, 259-260. <http://dx.doi.org/10.1134/1.1261837>
- [7] Appartaim, R., Mezonlin, E. D. and Johnson III, J.A. (2002) Turbulence in Plasma-Induced Hypersonic Drag Reduction. AIAA Journal , 40, 1979-1983. <http://dx.doi.org/10.2514/2.1559>
- [8] Joussot, R. and Viviana Lago, V. (2016) Experimental Investigation of the Properties of a Glow Discharge Used As Plasma Actuator Applied to Rarefied Supersonic Flow Control around a Flat Plate. IEEE Transactions on Dielectrics and Electrical Insulation, 23, 671-682. <http://dx.doi.org/10.1109/TDEI.2015.005327>
- [9] Kuo, S.P., Koretzky, E. and Orlick, L. (2001) Methods and Apparatus for Generating a Plasma Torch. United States Patent, US 6329628 B1.
- [10] Kuo, S.P., Kalkhoran, I.M., Bivolaru, D. and Orlick, L. (2000) Observation of Shock Wave Elimination by a Plasma in a Mach-2.5 Flow. Physics of Plasmas , 7, 1345-1348. <http://dx.doi.org/10.1063/1.873776>